

Intrinsic Gene Expression Profiles of Gliomas Are a Better Predictor of Survival than Histology

Lonneke A.M. Gravendeel,¹ Mathilde C.M. Kouwenhoven,¹ Olivier Gevaert,⁶ Johan J. de Rooi,^{2,3} Andrew P. Stubbs,² J. Elza Duijm,¹ Anneleen Daemen,⁶ Fonnet E. Bleeker,⁷ Linda B.C. Bralten,¹ Nanne K. Kloosterhof,^{1,5} Bart De Moor,⁶ Paul H.C. Eilers,³ Peter J. van der Spek,² Johan M. Kros,⁴ Peter A.E. Sillevs Smitt,¹ Martin J. van den Bent,¹ and Pim J. French¹

Departments of ¹Neurology, ²Bioinformatics, ³Biostatistics, and ⁴Pathology, Erasmus University Medical Center; ⁵Department of Pediatric Oncology and Hematology, Sophia Children's Hospital, Rotterdam, the Netherlands; ⁶Department of Electrical Engineering (ESAT-SCD), Katholieke Universiteit Leuven, Leuven, Belgium; and ⁷Department of Neurosurgery, Amsterdam Medical Center, Amsterdam, the Netherlands

Abstract

Gliomas are the most common primary brain tumors with heterogeneous morphology and variable prognosis. Treatment decisions in patients rely mainly on histologic classification and clinical parameters. However, differences between histologic subclasses and grades are subtle, and classifying gliomas is subject to a large interobserver variability. To improve current classification standards, we have performed gene expression profiling on a large cohort of glioma samples of all histologic subtypes and grades. We identified seven distinct molecular subgroups that correlate with survival. These include two favorable prognostic subgroups (median survival, >4.7 years), two with intermediate prognosis (median survival, 1–4 years), two with poor prognosis (median survival, <1 year), and one control group. The intrinsic molecular subtypes of glioma are different from histologic subgroups and correlate better to patient survival. The prognostic value of molecular subgroups was validated on five independent sample cohorts (The Cancer Genome Atlas, Repository for Molecular Brain Neoplasia Data, GSE12907, GSE4271, and Li and colleagues). The power of intrinsic subtyping is shown by its ability to identify a subset of prognostically favorable tumors within an external data set that contains only histologically confirmed glioblastomas (GBM). Specific genetic changes (epidermal growth factor receptor amplification, IDH1 mutation, and 1p/19q loss of heterozygosity) segregate in distinct molecular subgroups. We identified a subgroup with molecular features associated with secondary GBM, suggesting that different genetic changes drive gene expression profiles. Finally, we assessed response to treatment in molecular subgroups. Our data provide compelling evidence that expression profiling is a more accurate and objective method to classify gliomas than histo-

logic classification. Molecular classification therefore may aid diagnosis and can guide clinical decision making. [Cancer Res 2009;69(23):9065–72]

Introduction

Gliomas are the most common type of primary brain tumor in adults (1, 2). Despite advances in therapy, the prognosis for most glioma patients remains dismal. Based on their histologic appearance, gliomas can be divided into two major subtypes according to the 2007 WHO classification (1): astrocytic tumors, including pilocytic astrocytomas (PA), astrocytomas, and glioblastomas (GBM), and oligodendroglial (OD) tumors, including pure OD tumors and mixed oligoastrocytic (MOA) tumors. Tumors are further divided into grades I (PA), II (low grade), III (anaplastic), and IV (GBM) depending on the presence of anaplastic features (1). Patient survival, time to tumor progression, and response to therapy are all associated with subtype and grade of the tumor (1). In glioma patients, the histologic classification of tumors, often combined with perceived clinical prognostic features, guides treatment decisions. However, histologic classification of gliomas is troublesome and subject to interobserver variation (3).

Expression profiling provides an objective method to classify tumors (4, 5). Thus far, previous studies have shown that expression profiling correlates better with prognosis than histology (6) and may even be used to predict patients' prognosis (7–11). However, these studies have used external information (histology or clinical parameters) to build molecular classifiers. Furthermore, many studies were performed on a more restricted number of histologic diagnoses and/or tumor grades, contained incomplete clinical annotation, or included a relatively small number of patients (6–9, 12–19). Although these studies show that expression profiling can predict outcome based on supervised analysis, thus far only one study has identified intrinsic (unsupervised) subtypes of glioma and correlated them with patients' prognosis (20). However, no study has compared the prognostic and predictive value of molecular classification methods with that of histologic subtyping in glioma.

In this study, we therefore performed expression profiling on a large cohort of clinically annotated glioma samples of all histologic subtypes and grades. We provide strong evidence that the intrinsic molecular subtypes of gliomas correlate better with survival than histologic diagnosis. Furthermore, our data indicate that certain molecular subgroups clearly benefit from treatment. Our results

Note: Supplementary data for this article are available at Cancer Research Online (<http://cancerres.aacrjournals.org/>).

L.A.M. Gravendeel and M.C.M. Kouwenhoven contributed equally to this work.

Requests for reprints: Pim J. French, Department of Neurology, Erasmus University Medical Center, Room Be462a, P.O. Box 2040, 3000 CA Rotterdam, the Netherlands. Phone: 31-10-70-44-333; Fax: 31-10-70-44-465; E-mail: p.french@erasmusmc.nl.

©2009 American Association for Cancer Research.

doi:10.1158/0008-5472.CAN-09-2307

were validated on several large independent external data sets. Molecular classification therefore may aid diagnosis and may be used to guide clinical decision making.

Materials and Methods

Patients and tumor samples. Glioma samples were collected from the Erasmus University Medical Center tumor archive ($n = 276$) from patients (1989–2005), including seven repeat samples. Samples were collected immediately after surgical resection, snap frozen, and stored at -80°C . Use of patient material was approved by the Institutional Review Board. Medical history is stated in Supplementary Table S1. Survival time was defined as the period from date of surgery to date of death. If unavailable, date of last follow-up was used. Repeat samples were not included in survival analysis. All samples were visually inspected at the time of this study on their extent of tumor (J.M.K.). All histologic diagnoses were made on formalin-fixed, paraffin-embedded H&E sections and were reviewed (J.M.K.) blinded to the original diagnosis according to the 2007 WHO classification (1). GBMs were defined as secondary when symptoms occurred more than 1.5 y before histologic diagnosis or following relapse of a lower-grade glioma. Eight additional control samples (normal adult brain) were obtained from the Erasmus University Medical Center ($n = 4$) and the Dutch Brain Bank ($n = 3$) or purchased ($n = 1$; Qiagen).

Nucleic acid isolation, cDNA synthesis, and array hybridization. Total RNA and genomic DNA were isolated from 20 to 40 cryostat sections of 40- μm thickness using Trizol (Invitrogen) according to the manufacturer's instructions (14) and further purified on RNeasy mini columns (Qiagen). RNA quality was assessed on a Bioanalyzer (Agilent). One to two micrograms of high-quality RNA [i.e., RNA integrity number >6.5 (21)] was used for our experiments. Double-stranded cDNA synthesis and labeled cRNA synthesis were performed according to the Affymetrix Eukaryotic One-cycle cDNA synthesis protocol. Affymetrix HU133 Plus 2.0 microarrays were hybridized overnight with 10 μg of biotin-labeled cRNA. Genechips with a glyceraldehyde-3-phosphate dehydrogenase 5'/3' ratio >4 , present calls $<30\%$, unsuccessful RT controls, or a background >200 were excluded. Robustness of sample processing was assessed using eight biological replicates and three technical replicates. Replicates were not included in any analysis. Sample labeling and array hybridization on 250K *NspI* arrays was performed using high-quality genomic DNA according to the Genechip Mapping 500K Assay Manual ($n = 40$). Sample labeling and array hybridization on single-nucleotide polymorphism (SNP) 6.0 arrays were performed using Trizol-extracted, Repli-G (Qiagen)-amplified genomic DNA by AROS Applied Biotechnology AS according to standard Affymetrix protocols ($n = 15$).

Genetic aberrations. Loss of heterozygosity (LOH) of 1p19q was determined by microsatellite analysis or inferred from genotyping arrays. Microsatellites were amplified by PCR and analyzed as described (14). Allelic losses were statistically determined as described (22). Mutations in exon 4 of *IDH1* were determined by direct sequencing (Supplementary Table S2). Apart from experiments on 250K *NspI* arrays, all experiments used Trizol-extracted, Repli-G-amplified genomic DNA as starting material. Amplification of *EFGR* was determined by semiquantitative PCR as described (14).

Unsupervised clustering analysis. Expression levels of 17,527 genes were extracted from Affymetrix HU133 Plus 2.0 arrays using updated array annotation (23). Next, hierarchical ordered partitioning and collapsing hybrid (HOPACH) clustering was used to identify molecular subgroups in gliomas on 5,000 genes with highest variance (24). Nonparametric bootstrapping was used to estimate the probability that each sample belongs to a cluster (i.e., fuzzy clustering) and thus determine cluster stability. Samples were assigned to a cluster when at least 50% of bootstraps allocated the sample to that specific cluster.

The Cancer Genome Atlas (TCGA) and GSE4271 data sets used HU133A microarrays; thus, the actual probes used to define a probe set may differ between this and our data set. Cluster validation was performed by representing each of the molecular clusters in our data set by its centroid and classifying external samples to their nearest centroid. Samples belonging to

the original data set that were not assigned to a cluster were similarly assigned to the nearest centroid. Robustness of external validation was estimated with the in-group proportion (IGP) cluster quality measure (25). To validate the groups, the IGP scores are compared with a null distribution of IGPs. A P value for each IGP was calculated based on permutation tests. Both HOPACH and IGP were available as R packages.

Gene set enrichment analysis. Gene set enrichment analysis (GSEA) was done for each cluster versus the remaining samples against the MSigDB gene ontology gene sets (26, 27). Gene sets that are overexpressed or underexpressed in at least one cluster with P value of <0.01 and false discovery rate (FDR) q value of <0.05 were selected. Enrichment scores were calculated by the negative and positive logarithm (base 10) of the FDR q values for the overexpressed and underexpressed gene sets, respectively, such that overexpressed gene sets are scored on a positive scale and underexpressed gene sets on a negative scale.

Data analysis. Statistical processing of data was performed using Excel, Access, Stata 10.0, and Prism 5.02 (GraphPad). The significance of prognostic factors was determined with a multivariate analysis using Cox regression. Differences between Kaplan-Meier survival curves were calculated by the log-rank (Mantel-Cox) test. Comparisons between mean survivals of different groups were assessed by unpaired t tests, and comparisons between frequencies by the Fisher's exact test.

Results

Patient characteristics. A total of 276 glioma samples of following histology were included in this study: 8 astrocytomas grade 1 (PAs), 13 astrocytomas grade 2 (AII), 16 astrocytomas grade 3 (AIII), 159 astrocytomas grade 4 (GBM; 106 primary and 53 secondary), 28 MOAs (3 grade 2 and 25 grade 3), and 52 ODs (8 grade 2 and 44 grade 3). Male-to-female ratio was 2.1:1, median age at diagnosis was 50.2 years (range, 11.7–81.2), and mean Karnofsky performance score (KPS) was 78.9. Molecular clustering is an independent prognostic factor (Table 1) and remains independent when the analysis is performed on GBMs only (Supplementary Table S3). Age at time of diagnosis and KPS are well-documented prognostic factors in glioma (28–31). However, age at diagnosis does not remain an independent factor when taking molecular markers into account, as they mostly occur in tumor types associated with lower age at onset (*IDH1*, 1p19q). Due to the long period of inclusion, patients did not receive uniform treatment. One hundred and seventy-four (63%) patients were treated with radiotherapy and 24 (8.5%) with combined chemoradiation therapy, and a “wait and see” policy was applied to 11 (4%) patients until disease progression. Sixty-eight (24.5%) patients only received supportive treatment after diagnosis because of poor performance status, high age at diagnosis, rapid disease progression, or refusal of any other treatment by the patient. Detailed patient characteristics are listed in Supplementary Table S1.

Molecular clusters differ from histologic subgroups. Principle components analysis based on the 5,000 most variable genes in the data set highlights the relative difference and similarity between samples (Supplementary Fig. S1). Similar clustering results were obtained using all genes, half of the genes, or 1,000 genes. We then identified molecular subgroups in our data set based on similarities in gene expression levels between samples using the HOPACH algorithm. Twenty-four distinct molecular clusters were identified. Nonparametric bootstrapping confirmed that most samples indeed belong to a defined cluster (fuzzy clustering). Only 17 samples were assigned to a cluster different from the original after bootstrapping, indicating the high stability of the clusters (see Materials and Methods). More specifically, all of these samples had very sparse cluster memberships, meaning

Table 1. Multivariate analysis (Cox regression analysis) on all samples

	Hazard ratio	SE	z	P > [z]	95% Confidence interval
Molecular cluster	1.43	0.205	2.51	0.012	1.081–1.896
Histologic type	0.72	0.192	-1.24	0.216	0.425–1.213
Histologic grade	0.67	0.439	-0.62	0.537	0.182–2.428
KPS	0.96	0.019	-2.32	0.02	0.920–0.993
Age at diagnosis	1.01	0.019	0.33	0.744	0.970–1.044
Sex	0.35	0.145	-2.53	0.011	0.155–0.789
Extent of surgery	0.67	0.147	-1.84	0.066	0.432–1.028
Chemotherapy	0.90	0.090	-1.03	0.304	0.741–1.098
EGFR amplification	1.22	0.318	0.75	0.451	0.730–2.031
LOH 1p	0.37	0.382	-0.96	0.336	0.050–2.782
LOH 19q	2.29	2.107	0.9	0.368	0.377–13.898
IDH1 mutation	0.55	0.272	-1.21	0.225	0.206–1.451

that for most of these samples the remaining cluster membership was to one or very few clusters. Clustering of samples and bootstrapping results are shown in Supplementary Fig. S2 and Supplementary Table S4.

We then focused our analysis on the five largest clusters containing >10 samples each (clusters 9, 16, 17, 22, and 23) and two smaller subgroups that are molecularly (Supplementary Fig. S1) and histologically distinct: a control sample cluster 0 (*n* = 8; a merge of clusters 0, 1, and 3) and cluster 16 that contains PAs (*n* = 6; a merge of clusters 14, 15, and 16) and 3 recurrences of PAs. All samples were

then reassigned to one of these seven clusters. After reassignment, clusters 0, 9, 16, 17, 18, 22, and 23 contained 23, 44, 10, 38, 64, 26, and 79 samples, respectively.

All clusters contain a wide variety of histologic diagnosis and malignancy grades. However, distinct histologic subtypes segregate into different molecular clusters. For example, clusters 18, 22, and 23 predominantly contain GBMs; cluster 9 contains most of the ODs (grade 2 and 3); and six of eight PAs cluster in group 16. Cluster 17 is the most histologically diverse cluster. The histologic composition of all molecular subgroups is shown in Fig. 1A.

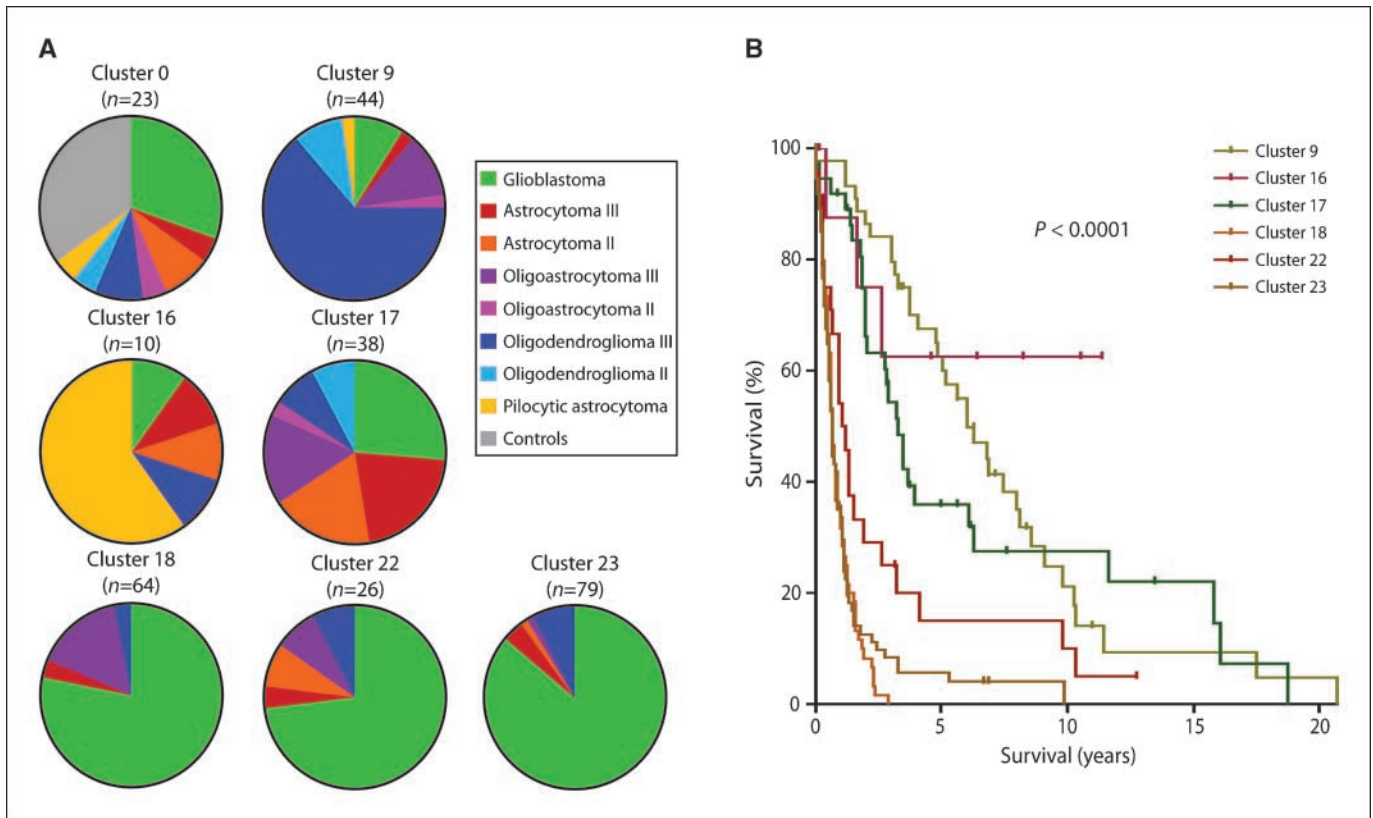


Figure 1. Molecular subgroups are distinct from histologic subgroups and correlate with survival. *A*, composition of individual molecular subgroups by their histologic subtypes. Each molecular subgroup is composed of a variety of different histologic subtypes, although distinct histologic subtypes predominate distinct molecular subgroups. *B*, Kaplan-Meier survival analysis of molecular clusters. Intrinsic gene expression profiles identify two molecular clusters with poor prognosis (18 and 23), two with intermediate prognosis (17 and 22), and two with relatively favorable prognosis (9 and 16).

Table 2. Clinical characteristics of the molecular subgroups

	Cluster 9	Cluster 16	Cluster 17	Cluster 18	Cluster 22	Cluster 23
Median age at diagnosis (y)	48.50	36.50	38.30	58.00	46.00	54.70
Median survival (y)	6.06	Undefined	3.32	0.68	1.12	0.67
Mean KPS	82.9	70.9	89.2	77.0	79.2	79.7

NOTE: Median age at diagnosis, median survival, and mean KPS per molecular cluster. Median survival of cluster 16 could not be defined because 6 of 10 patients were still alive at time of last follow-up.

Because control brain samples are markedly different in gene expression profile from the large majority of glioma samples (Supplementary Fig. S1), we were surprised that cluster 0 contained 15 glioma samples in addition to the 8 control brain samples. We hypothesized that the tumor samples in cluster 0 might contain a large amount of nonneoplastic tissue. Indeed, histologic reexamination of all samples by a blinded experienced neuropathologist (J.M.K.) confirmed that all 15 samples that were reassigned to cluster 0, but none of the other samples, contained a substantial (>50%) amount of nonneoplastic brain tissue. Because of the high amount of nonneoplastic tissue in the samples in this cluster, we were unable to extract a clear glioma-derived expression profile and, therefore, did not involve cluster 0 in the survival analysis.

Molecular clusters correlate with survival. Kaplan-Meier survival analysis highlighted that the molecular clusters differ significantly with respect to their survival ($P < 0.0001$). As

illustrated in Fig. 1B, molecular clusters are separated in two favorable prognostic subgroups (9 and 16; median survival of 6.06 and >4.7 years, respectively), two subgroups with intermediate prognosis (17 and 22; median survival of 1.1 and 3.32 years, respectively), and two subgroups with poor prognosis (18 and 23; median survival of 0.68 and 0.67 years, respectively). Cluster 16 has a median survival of >4.7 years, as 6 of 10 patients were still alive at the time of last follow-up. Clinical characteristics of the molecular subgroups are summarized in Table 2. In repeat samples, cluster assignment either remained identical or changed to a molecular subgroup with poorer prognosis (Supplementary Table S5).

Cox regression analysis showed that molecular clustering is an independent significant prognostic variable in survival ($P < 0.012$; Table 1). Other factors in survival are age at diagnosis, KPS, and sex (28–31). These results are illustrated by Supplementary Fig. S3 and show that additional prognostic factors can help estimate prognosis.

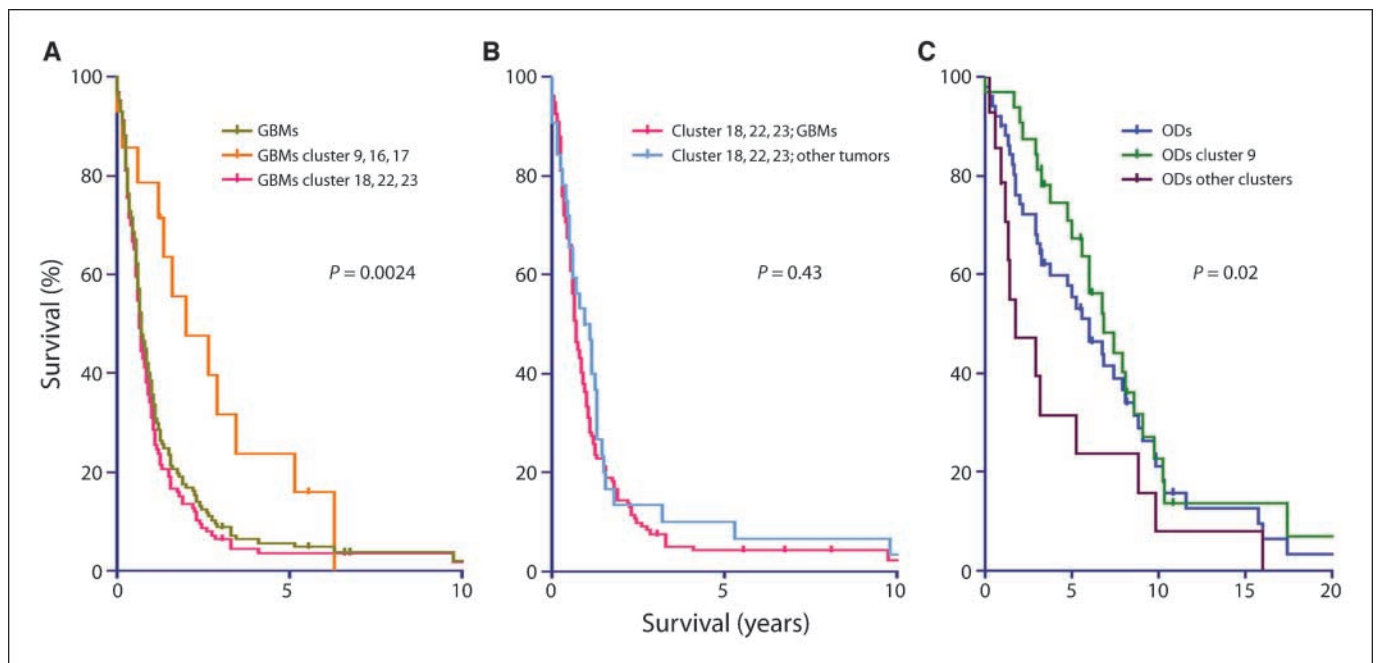
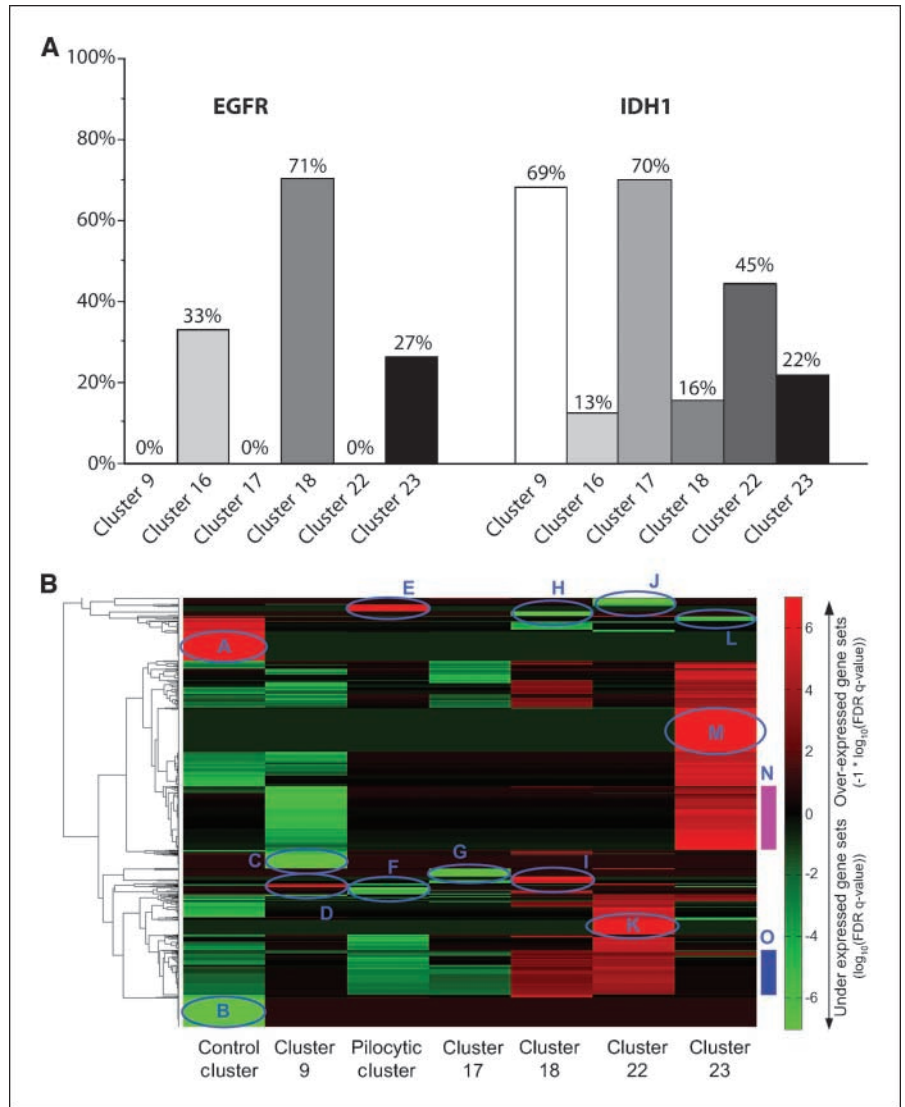


Figure 2. Molecular subgroups correlate better with survival than histologic subgroups. Comparison between molecular and histologic classification. *A*, samples of the same histologic diagnosis (GBM) were separated by their molecular profile into those present in poorest prognostic molecular subgroups (18, 22, and 23) and those present in relatively favorable prognostic molecular subgroups (9, 16, and 17). The median survival of all GBMs was 0.73 y, but patients with a GBM in a poor molecular subgroup perform worse than patients with a GBM in a relatively favorable subgroup (0.70 versus 2.1 y; $P < 0.01$). *B*, samples present in poor molecular subgroups (median survival, 0.82 y) cannot be further separated by their histologic appearance into those of poor (GBMs) and less poor (all other tumors) prognostic subgroups (median survival, 0.71 and 1.04 y). *C*, similar to *A* but using ODIs and ODIIIs as histologic subgroup (median survival, 6.04 y) further separated by their poor and relatively favorable molecular subgroup (median survival, 6.87 and 1.78 y; $P < 0.023$). These results show that molecular clustering has additional prognostic value to histologic diagnosis, whereas histologic diagnosis does not have additional prognostic value to molecular subgroups.

Figure 3. Genetic and pathway differences between molecular subgroups. *A*, distinct genetic changes are associated with distinct molecular clusters. Amplification of *EGFR* is predominantly observed in clusters 18 and 23, whereas mutations in *IDH1* are more prevalent in clusters 9 and 17. These data strongly suggest that distinct molecular subtypes have different underlying causal genetic changes. *B*, clustering of GSEA scores. *A* to *O* correspond to gene set clusters that are differentially expressed in at least one subtype. These functional categories were investigated by extracting overlapping genes in >10% of all gene sets in a particular cluster. Functional categories: *A*, cyclic AMP binding, neurogenesis, GnRH signaling, long-term potentiation; *B*, protein transport and regulation; *C*, no significant functional categories; *D*, ribosome, metabolic processes, histone and chromatin modification, RNA transcription; *E*, fatty acid metabolism; *F*, oxidative phosphorylation, transport; *G*, no significant functional categories; *H*, G-protein coupled receptor, neuropeptide binding; *I*, RNA polymerase and transcription; *J*, amino acid transport; *K*, ribosome, mitochondrion; *L*, cell-cell signaling, nervous system development, ion channel activity; *M*, immune response; *N*, Janus-activated kinase–signal transducer and activator of transcription signaling, response to stress and wounding, apoptosis, immune response; *O*, cell cycle, mitosis, response to DNA damage.



Molecular clusters correlate better with patient survival than histologic subgroups. Because histology also correlates with patient survival, we compared the accuracy of survival prediction by the two classification methods. To this end, we separated samples of the same histologic diagnosis by their molecular profile. Conversely, samples of the same molecular subgroup were further separated by their histologic appearance. The median survival of all GBMs used in our study was 0.73 years (range, 0.02–9.8). However, GBMs in the three poorest prognostic molecular subgroups (18, 22, and 23) have a significantly shorter median survival compared with GBMs in the three most favorable molecular clusters (9, 16, and 17; 0.70 versus 2.05 years; $P = 0.0024$; Fig. 2*A*). Conversely, within the poor prognostic subgroups (18, 22, and 23), no significant difference was observed in median survival between samples with poorest histologic diagnosis (GBM) versus those with a histologically more favorable prognosis (all non-GBM; Fig. 2*B*). Similar to GBMs, ODs in the favorable molecular cluster 9 have a significantly better prognosis than the ODs in the poor prognostic subgroups ($P = 0.02$; Fig. 2*C*). Our data show that unsupervised molecular clustering has additional prognostic value to histologic diagnosis, whereas histologic diagnosis does not add prognostic value to

molecular subgroups. The intrinsic molecular subtypes of glioma therefore predict survival more accurately than histology in our data set.

Molecular analysis. We next evaluated the frequencies of known molecular markers in gliomas within the subgroups. LOH of 1p19q was determined in 149 of 276 (54%) samples. Virtually all samples in cluster 9 have LOH on 1p (85%) or on 19q (85%; regardless of histology), with 82% of samples showing combined loss. 1p/19q LOH was observed at significantly lower frequencies in samples not associated with cluster 9, with 11% showing combined loss ($P < 0.0001$, Fisher's exact test). Epidermal growth factor receptor (*EGFR*) status was determined in 151 (55%) samples (unbiased toward histologic diagnosis). *EGFR* amplification was predominantly observed in clusters 18 and 23 (71%; 27%); no amplification was seen in clusters 9, 17, and 22. Sequencing of *IDH1* exon 4 was successfully evaluated in 226 (82%) cases. Mutations in the highly conserved Arg¹³² were predominantly identified in clusters 9 (69%) and 17 (70%). Clusters 16, 18, 22, and 23 contained 13%, 16%, 45%, and 22% R132 mutations, respectively. A complete overview of genetic changes is stated in Fig. 3*A* and Supplementary Table S6.

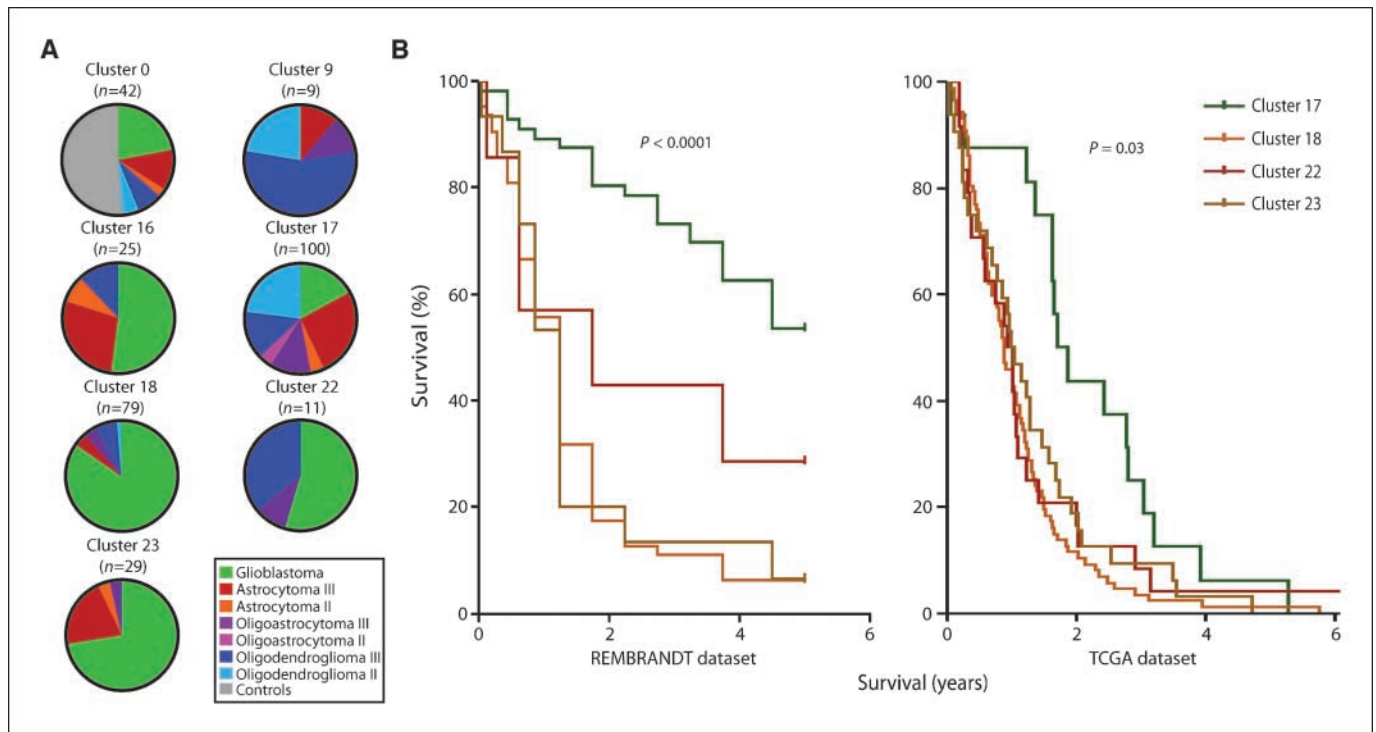


Figure 4. Molecular subgroups can be confirmed in external data sets. **A**, composition of individual molecular subgroups by their histologic subtype. Each molecular subgroup is composed of a variety of different histologic subtypes in the REMBRANDT data set. Similar to our set, histologic subtypes predominate distinct molecular subgroups. **B**, Kaplan-Meier survival analysis of molecular clusters in the REMBRANDT data set (*left*) and the TCGA data set (*right*). Both sets show similar trends in survival compared with our data.

Figure 3B shows the clustering of the GSEA enrichment scores using average linkage hierarchical clustering using cosine similarity. Our data show that each molecular subgroup has a distinct pattern of genetic changes.

Cluster validation. Five independent external data sets were used to validate our clustering results: The Cancer Genome Atlas⁸ data set ($n = 236$; ref. 12), the Repository for Molecular Brain Neoplasia Data⁹ data set [REMBRANDT; $n = 296$; National Cancer Institute (2005), assessed 2008 December; ref. 32], a data set containing 21 PAs (GSE12907; ref. 33), data set GSE4271 (8), and a data set from a recent study (20). In all cases, the molecular clustering results correlate with the composition of the data set. For example, the TCGA data set only consists of GBMs, which is reflected by the predominance of clusters 18, 22, and 23. The REMBRANDT data set has a more diverse histologic makeup (ODs, MOAs, astrocytomas, and GBMs), which is reflected by the recurrence of all molecular clusters (Fig. 4A). Finally, GEO data set GSE12907 contains 21 PAs, which is reflected by 20 of 21 samples being grouped in cluster 16.

When comparing the survival of molecular clusters in both the TCGA and REMBRANDT data sets, the relative differences between molecular subgroups are virtually identical to those identified in our data set (Fig. 4B). For example, clusters 9 and 17 have significantly longer median survival in the REMBRANDT data set compared with clusters 18, 22, and 23 ($P < 0.0001$). Eighteen of the GBM samples in the TCGA data set were assigned to the relatively more favorable molecular cluster 17. These patients indeed had signifi-

cantly longer survival (799 days) compared with those of clusters 18, 22, and 23 (420 days; $P = 0.0002$). Only one GBM sample of the TCGA data set was assigned to cluster 9. This patient had the longest survival in the entire data set (9.7 years). The identification of prognostically favorable samples in a data set that contains only GBMs highlights the prognostic power of intrinsic expression profiles.

Analysis of genetic changes in the TCGA data set showed that both *EGFR* amplification and *IDH1* mutation frequencies have virtually identical distribution across the different subgroups (Supplementary Fig. S4; refs. 12, 34). Distributions of other frequently mutated genes (*NF1* and *P53*) are shown in Supplementary Fig. S5. Furthermore, the single patient assigned to cluster 9 in the TCGA data set indeed showed LOH on 1p19q (34), as did one of the samples from the REMBRANDT data set assigned to cluster 9. SNP chip data were not available for other samples of the REMBRANDT data set assigned to cluster 9. In summary, the intrinsic glioma subgroups identified in our study can be validated in external data sets with respect to histologic, molecular, and clinical features.

We overlaid our clustering results onto GSE4271 (8), which again resulted in similar survival between molecular subgroups (Supplementary Fig. S6). The three different signatures identified by Phillips and colleagues (proneural, proliferative, and mesenchymal; see also ref. 35) segregated into specific molecular subgroups. For example, the proneural signature was predominantly found in clusters 16 and 17, whereas the proliferative and the mesenchymal signatures were mostly found in clusters 18, 22, and 23 (Supplementary Fig. S7A). Conversely, these results are confirmed when imposing these signatures onto our data set (Supplementary Fig. S7B). However, one of our best prognostic groups (cluster 9) is classified as poor prognostic group (proliferative) by Phillips and

⁸ <http://cancergenome.nih.gov>

⁹ <http://rembrandt.nci.nih.gov>

colleagues. This shows that, at least for some molecular subtypes, our clustering method predicts prognosis more specifically. Li and colleagues (20) also identified intrinsic molecular subtypes of gliomas by expression profiling. These subgroups can be confirmed in our data set, with similar survival to reported (Supplementary Fig. S8A). However, samples in the poor prognostic subgroup identified by Li and colleagues (G-groups) can be further separated based on our molecular classification into a poor prognostic group ($n = 132$) and a more favorable prognostic group ($n = 18$) with significantly better survival ($P = 0.03$; Supplementary Fig. S8B). Similarly, samples that cluster in good prognostic subgroups of Li and colleagues (OA and OB group) can be separated by our profiles into a poor prognostic group ($n = 13$) and a favorable prognostic group ($n = 67$; $P = 0.009$; Supplementary Fig. S8C). The reverse analysis is shown in Supplementary Fig. S9. GSEA shows that some of the pathways identified by Li and colleagues show differential distribution in our subgroups (Supplementary Fig. S10). This indicates that the different clustering methods show some overlap.

Molecular clusters and treatment response. Finally, we examined whether there are differences in treatment response between molecular subgroups. The efficacy of treatment in molecular subgroups could be assessed in our sample cohort as patients were treated heterogeneously. A clear effect of radiotherapy was observed in clusters 18 and 23 ($P < 0.001$ and $P = 0.01$, respectively). In other clusters, the effects were either less pronounced or contained too few samples to reach statistical significance. However, to eliminate potential effects of sample bias, we used an external data set (GSE7696; ref. 16) that consisted of 80 GBM patients from a randomized controlled trial in which patients were treated with radiotherapy versus combined chemoradiation. We identified the following molecular clusters in this data set: clusters 0 ($n = 4$), 16 ($n = 3$), 17 ($n = 10$), 18 ($n = 52$), 22 ($n = 4$), and 23 ($n = 11$; Supplementary Fig. S11A). Results showed that both clusters 18 and 23 seem to benefit from combined chemoradiation therapy (Supplementary Fig. S11B) compared with radiotherapy only. Other clusters contain too few samples to assess effect of treatment.

Discussion

In this study, we have examined whether expression profiling can serve as a more objective method to classify gliomas than histology. Our data show that expression profiling identifies molecular subgroups that are distinct from histologic subgroups and that these molecular subgroups correlate better with patient survival. In addition, our data indicate that distinct molecular subgroups benefit from treatment. As a confirmatory step, the molecular subgroups and their prognostic values were validated on five independent sample cohorts. Finally, specific genetic changes (*EGFR* amplification, *IDH1* mutation, and 1p19q LOH) segregate in distinct molecular subgroups.

At present, the treatment pathway for glioma patients has been optimized for the different histologic subtypes. However, classification based on histologic appearance has a high degree of interobserver variability (3). The intrinsic subtypes of glioma identified in our study therefore provide a robust and objective alternative to histologic classification. The power of intrinsic subtyping was shown by its ability to identify a subset of prognostically favorable tumors within an external data set that contains only histologically confirmed GBMs (TCGA).

Distinct genetic changes segregate into different intrinsic molecular clusters. For example, amplification of *EGFR* is predominantly observed in clusters 18 and 23, whereas mutations in *IDH1* are sig-

nificantly more prevalent in clusters 9 and 17. All but four samples in cluster 9 have LOH on 1p19q regardless of histologic subtype. This observation is confirmed in external data sets.

Interestingly, the molecular changes and clinical features associated with secondary GBMs (high mutation rate of *IDH1*, absent *EGFR* amplification, and lower age at time of diagnosis) are reflected in a distinct molecular subgroup (cluster 22) that indeed is enriched in the number of secondary GBMs. Differences in genetic changes between molecular subtypes can indicate that novel targeted agents may only be effective in distinct molecular subtypes (Supplementary Fig. S12).

Cluster 0 contains all nonneoplastic tissue samples in our study ($n = 8$), in the REMBRANDT data set ($n = 21$), and in GSE7696 ($n = 4$). However, cluster 0 also contains several glioma samples in our data set ($n = 15$), in the TCGA data set ($n = 3$), and in the REMBRANDT data set ($n = 20$). In our data set, samples that are associated with cluster 0 have significant amounts of nonneoplastic tissue (>50%). Similarly, two of three samples of the TCGA data set contained >90% nonneoplastic tissue (data on other sample not available) and have virtually no genetic aberrations. The samples of the REMBRANDT data set that associate with cluster 0 might therefore also contain substantial amounts of nontumor tissue.

Our data indicate that both clusters 18 and 23 benefit from chemoradiation. This benefit seems to be reflected by an increase in overall survival between our data set, in which few samples received chemoradiation, and the TCGA, in which most samples received chemoradiation (0.68 versus 0.89 years and 0.67 versus 1.02 years in clusters 18 and 23, respectively). However, in the TCGA data set, cluster 22 does not show improved survival (1.1 versus 0.98 years), and it is possible that current treatment standards do not affect this specific molecular subgroup. Unfortunately, too few samples from this chemoradiotherapy (16) were assigned to cluster 22 to assess treatment efficacy.

Another study also identified intrinsic molecular subtypes of gliomas by expression profiling (20). Although these molecular clusters also correlate with patient survival, a comparison with histologic diagnosis and molecular markers was not attempted. In addition, several histologic subtypes were not included (control tissue, MOAs, and PAs) in building molecular glioma classifiers. Our data show that our molecular clustering has additional prognostic value both to histologic diagnosis (20) and to alternative clustering methods (8, 20).

There are several limitations using unsupervised hierarchical clustering for subclassification based on mRNA expression profiles. For example, tumor types that are not included in present study (e.g., brain metastasis) and rare tumor types with insufficient sample size to form a separate molecular cluster will be incorrectly classified. Histologic examination to detect such histologies therefore remains required. To some extent, molecular cluster definition also depends on the algorithms used (both for clustering and data extraction) so that individual samples may switch between molecular subgroups.

In conclusion, our data indicate that the intrinsic subtypes identified improve on histologic classification of gliomas and are an accurate predictor of prognosis. Molecular classification can contribute to diagnosis and may form a rationale for clinical decision making and novel targeted therapies.

Disclosure of Potential Conflicts of Interest

No potential conflicts of interest were disclosed.

Acknowledgments

Received 6/23/09; revised 9/1/09; accepted 9/19/09; published OnlineFirst 11/17/2009.

Grant support: Novartis AG (Basel); Erasmus University Medical Center MRACE grants 2006 (L.B.C. Bralten) and 2007 (N.K. Kloosterhof); IWT-Vlaanderen (O. Gevaert); FWO (A. Daemen); BDM Research Council KUL; GOA AMBioRICS, CoE EF/05/007 SymBioSys, PROMETA, FWO: G.0499.04, G.0302.07 (ICCoS, ANMMM, MLDM); G.082409. IWT: PhD Grants, SBO-BioFrame, BFSPO: IUAP P6/25 (BioMaGNet, 2007-2011); EU-RTD: ERNSI; FP6-NoE Biopattern; and FP6-IP e-Tumours, FP6-MC-EST Bioptrain.

The costs of publication of this article were defrayed in part by the payment of page charges. This article must therefore be hereby marked *advertisement* in accordance with 18 U.S.C. Section 1734 solely to indicate this fact.

We thank O. Groeneveld for his help with sequencing on IDH1.

The results published here are in part based on data generated by The Cancer Genome Atlas (TCGA) pilot project established by the NHI and National Human Genome Research Institute. Information about TCGA and the investigators and institutions who constitute the TCGA research network can be found at their Web site (<http://cancergenome.nih.gov>).

References

- Louis DN, Ohgaki H, Wiestler OD, Cavenee WK, editors. WHO classification of tumours of the central nervous system. 4th ed. Lyon: WHO; 2007.
- Ohgaki H, Dessen P, Jourde B, et al. Genetic pathways to glioblastoma: a population-based study. *Cancer Res* 2004;64:6892-9.
- Kros JM, Gorlia T, Kouwenhoven MC, et al. Panel review of anaplastic oligodendroglioma from European Organization For Research and Treatment of Cancer Trial 26951: assessment of consensus in diagnosis, influence of 1p/19q loss, and correlations with outcome. *J Neuropathol Exp Neurol* 2007;66:545-51.
- Sorlie T, Perou CM, Tibshirani R, et al. Gene expression patterns of breast carcinomas distinguish tumor subclasses with clinical implications. *Proc Natl Acad Sci U S A* 2001;98:10869-74.
- Valk PJ, Verhaak RG, Beijen MA, et al. Prognostically useful gene-expression profiles in acute myeloid leukemia. *N Engl J Med* 2004;350:1617-28.
- Nutt CL, Mani DR, Betensky RA, et al. Gene expression-based classification of malignant gliomas correlates better with survival than histological classification. *Cancer Res* 2003;63:1602-7.
- Shirahata M, Iwao-Koizumi K, Saito S, et al. Gene expression-based molecular diagnostic system for malignant gliomas is superior to histological diagnosis. *Clin Cancer Res* 2007;13:7341-56.
- Phillips HS, Kharbanda S, Chen R, et al. Molecular subclasses of high-grade glioma predict prognosis, delineate a pattern of disease progression, and resemble stages in neurogenesis. *Cancer Cell* 2006;9:157-73.
- Freije WA, Castro-Vargas FE, Fang Z, et al. Gene expression profiling of gliomas strongly predicts survival. *Cancer Res* 2004;64:6503-10.
- Shirahata M, Oba S, Iwao-Koizumi K, et al. Using gene expression profiling to identify a prognostic molecular spectrum in gliomas. *Cancer Sci* 2009;100:165-72.
- Petalidis LP, Oulas A, Backlund M, et al. Improved grading and survival prediction of human astrocytic brain tumors by artificial neural network analysis of gene expression microarray data. *Mol Cancer Ther* 2008;7:1013-24.
- TCGARN. Comprehensive genomic characterization defines human glioblastoma genes and core pathways. *Nature* 2008;455:1061-8.
- Parsons DW, Jones S, Zhang X, et al. An integrated genomic analysis of human glioblastoma multiforme. *Science* 2008;321:1807-12.
- French PJ, Swagemakers SM, Nagel JH, et al. Gene expression profiles associated with treatment response in oligodendrogliomas. *Cancer Res* 2005;65:11335-44.
- French PJ, Peeters J, Horsman S, et al. Identification of differentially regulated splice variants and novel exons in glial brain tumors using exon expression arrays. *Cancer Res* 2007;67:5635-42.
- Murat A, Migliavacca E, Gorlia T, et al. Stem cell-related "self-renewal" signature and high epidermal growth factor receptor expression associated with resistance to concomitant chemoradiotherapy in glioblastoma. *J Clin Oncol* 2008;26:3015-24.
- Liang Y, Diehn M, Watson N, et al. Gene expression profiling reveals molecularly and clinically distinct subtypes of glioblastoma multiforme. *Proc Natl Acad Sci U S A* 2005;102:5814-9.
- Nigro JM, Misra A, Zhang L, et al. Integrated array-comparative genomic hybridization and expression array profiles identify clinically relevant molecular subtypes of glioblastoma. *Cancer Res* 2005;65:1678-86.
- Tso CL, Shintaku P, Chen J, et al. Primary glioblastomas express mesenchymal stem-like properties. *Mol Cancer Res* 2006;4:607-19.
- Li A, Walling J, Ahn S, et al. Unsupervised analysis of transcriptomic profiles reveals six glioma subtypes. *Cancer Res* 2009;69:2091-9.
- Schroeder A, Mueller O, Stocker S, et al. The RIN: an RNA integrity number for assigning integrity values to RNA measurements. *BMC Mol Biol* 2006;7:3.
- Harkes IC, Elstrodt F, Dinjens WN, et al. Allelotype of 28 human breast cancer cell lines and xenografts. *Br J Cancer* 2003;89:2289-92.
- Dai M, Wang P, Boyd AD, et al. Evolving gene/transcript definitions significantly alter the interpretation of GeneChip data. *Nucleic Acids Res* 2005;33:e175.
- van der Laan M, Pollard KS. A new algorithm for hybrid hierarchical clustering with visualization and the bootstrap. *J Stat Plan Infer* 2002;117:275-303.
- Kapp AV, Tibshirani R. Are clusters found in one dataset present in another dataset? *Biostatistics* 2007;8:9-31.
- Subramanian A, Tamayo P, Mootha VK, et al. Gene set enrichment analysis: a knowledge-based approach for interpreting genome-wide expression profiles. *Proc Natl Acad Sci U S A* 2005;102:15545-50.
- Dennis G, Jr., Sherman BT, Hosack DA, et al. DAVID: Database for Annotation, Visualization, and Integrated Discovery. *Genome Biol* 2003;4:P3.
- Tortosa A, Vinolas N, Villa S, et al. Prognostic implication of clinical, radiologic, and pathologic features in patients with anaplastic gliomas. *Cancer* 2003;97:1063-71.
- Showalter TN, Andrej J, Andrews DW, Curran WJ, Jr., Daskalakis C, Werner-Wasik M. Multifocal glioblastoma multiforme: prognostic factors and patterns of progression. *Int J Radiat Oncol Biol Phys* 2007;69:820-4.
- Curran WJ, Jr., Scott CB, Horton J, et al. Recursive partitioning analysis of prognostic factors in three Radiation Therapy Oncology Group malignant glioma trials. *J Natl Cancer Inst* 1993;85:704-10.
- Pignatti F, van den Bent M, Curran D, et al. Prognostic factors for survival in adult patients with cerebral low-grade glioma. *J Clin Oncol* 2002;20:2076-84.
- Madhavan S, Zenklusen JC, Kotliarov Y, Sahni H, Fine HA, Buetow K. Rembrandt: helping personalized medicine become a reality through integrative translational research. *Mol Cancer Res* 2009;7:157-67.
- Wong KK, Chang YM, Tsang YT, et al. Expression analysis of juvenile pilocytic astrocytomas by oligonucleotide microarray reveals two potential subgroups. *Cancer Res* 2005;65:76-84.
- Freire P, Vilela M, Deus H, et al. Exploratory analysis of the copy number alterations in glioblastoma multiforme. *PLoS ONE* 2008;3:e4076.
- Lee Y, Scheck AC, Cloughesy TF, et al. Gene expression analysis of glioblastomas identifies the major molecular basis for the prognostic benefit of younger age. *BMC Med Genomics* 2008;1:52.